Construction and Manipulation of Functional Three-Dimensional Droplet Networks

Tobias Wauer,[†,§] Holger Gerlach,[†] Shiksha Mantri,[†,⊥] Jamie Hill,[‡] Hagan Bayley,[†] and K. Tanuj Sapra[†,∥,*]

[†]Department of Chemistry, University of Oxford, Oxford OX1 3TA, United Kingdom and [‡]Life Science Interface Doctoral Training Programme, Rex Richards Building, University of Oxford, Oxford OX1 3QU, United Kingdom. [§]Present address: MRC Laboratory of Molecular Biology, Francis Crick Avenue, CB2 0QH, Cambridge, UK. [⊥]Present address: Laboratory of Organic Chemistry, HCI F 335, Wolfgang-Pauli-Strasse 10, 8093 Zurich, Switzerland. [∥]Present address: Department of Biochemistry, University of Zurich, Winterthurerstrasse 190, 8057 Zurich, Switzerland.

ABSTRACT Previously, we reported the manual assembly of lipid-coated aqueous droplets in oil to form two-dimensional (2D) networks in which the droplets are connected through single lipid bilayers. Here we assemble lipid-coated droplets in robust, free-standing 3D geometries: for example, a 14-droplet pyramidal assembly. The networks are designed, and each droplet is placed in a designated position. When protein pores are inserted in the bilayers between specific constituent droplets, electrical and chemical communication pathways are generated. We further describe an improved means to construct 3D droplet networks with defined organizations by the manipulation of aqueous droplets containing encapsulated magnetic beads. The droplets are maneuvered in a magnetic field to form simple construction modules, which are then used to form larger 2D and 3D structures including a 10-droplet pyramid. A methodology to construct freestanding, functional 3D droplet networks is an important step toward the programmed and automated manufacture of synthetic minimal tissues.

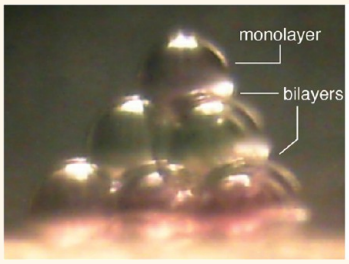

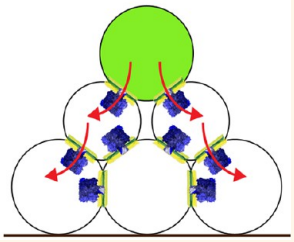

KEYWORDS: 3D assembly · communication · droplets · lipid bilayers · magnetic manipulation · networks · synthetic biology

Aqueous droplets have been used as miniature compartments for down-scaling manipulations in molecular biology,[1,2] for diagnostic[3] and screening applications,[4] and even to understand the origins of life.[5,6] For example, droplets have been used to increase the scale and throughput of directed evolution experiments.[7,8] Lipid bilayer-encapsulated droplets akin to biological cells and cellular compartments have been made in the form of attoliter (aL)- to nanoliter (nL)-sized liposomes and giant unilamellar vesicles[9] and used as minimal cells in synthetic biology.[10−12] Recently, a new system based on lipid-encapsulated aqueous droplets in oil has been developed; two lipid-coated droplets when brought into contact form a lipid bilayer. The bilayer can host membrane pores and ion channels and is stable in an applied electrical potential enabling the measurement of ionic currents.[13,14] Useful applications of droplet interface bilayers (DIB) and droplet networks have been realized in synthetic biology and bionanotechnology.[15] Combined with engineered α-hemolysin (αHL) protein nanopores, the droplet system has been used to construct functional devices such as a light sensor, a biobattery,[13] and current rectifiers.[16] In the context of synthetic biology, droplets are attractive minimal cells,[17] and by extension, droplet networks are potential minimal tissues.[15,18] Recently, it was shown that droplet bilayers, encapsulated in an oil drop, are able to communicate with an external aqueous medium through αHL pores,[19] allowing the networks to be used in a physiological environment.

Here, to develop droplet networks further for applications in biotechnology and synthetic biology, we have formed free-standing 3D networks, capable of internal communication, *i.e.*, able to transmit chemical and electrical signals between compartments along predefined paths. The 3D tissue morphologies found in nature are more spatially economical than their 2D counterparts, affording shorter and quicker

* Address correspondence to k.sapra@bioc.uzh.ch.

Received for review October 17, 2013 and accepted December 16, 2013.

Published online December 16, 2013
10.1021/nn405433y

communication paths between cells. A further key advance would be the ability to construct droplet networks automatically in a precisely controlled manner and further manipulate the individual droplets and the entire assembly noninvasively. Here, we demonstrate that a magnetic field can be used to manipulate lipid-coated droplets with sub-millimeter precision to form 2D and 3D droplet networks in a modular fashion.

RESULTS AND DISCUSSION

Manual Assembly of 3D Droplet Networks. Three-dimensional droplet networks were formed in various geometries (Figure 1). The 3D assemblies were constructed manually by pipetting aqueous droplets of 80−200 nL into oil containing 1,2-diphytanoyl-*sn*-glycero-3-phosphocholine (DPhPC) and incubating them to allow a lipid monolayer to form. A lower 2D layer of droplets was then brought together by using a pipet tip. To form a 3D network, droplets were sucked into a pipet tip and released carefully onto the 2D assembly. A mixture of silicone oil and hexadecane (1:1 v/v; see Methods) was found to increase the bilayer stability. The formation of stable bilayers was crucial to prevent droplets from fusing and to avoid the slippage of upper droplets. Top droplets sat neatly in the crevice formed by the bilayer interface of the droplets at the bottom. The bottom bilayers were able to support the weight of the top droplet (Figure 1).

Functional 3D Networks. Owing to the presence of an interface bilayer, it is possible to establish communication between two droplets with the help of membrane pores such as α-hemolysin. However, the exchange of contents between two droplets, with intervening droplets, will take a long time due to diffusion-limited transfer. Arranging droplets in 3D may be a good way to decrease the distance between two droplets and at the same time increase the number of bilayer connections (Supplementary Note 1).

In one example, a 10-droplet pyramidal network with specific signaling pathways was constructed (Figure 1b, Figure 2, and Figure S1). One droplet (α) contained a high concentration of wild-type α-hemolysin (WT αHL) heptamer, and another droplet contained γ-cyclodextrin (γCD). A "probe" droplet (β) with a lower concentration of αHL was suspended from the end of a Ag/AgCl electrode (*trans*) (see Methods) to detect ionic paths through the network droplets measured as electrical signals. The probe droplet was used to form bilayers sequentially with different droplets in each of the three layers of the pyramid. A lipid bilayer formed between the probe droplet and a droplet in the 3D assembly was undone by slowly retracting the probe droplet by using the micromanipulator. Upon touching droplet β to different droplets in the assembly, ion flow was detected through droplet bilayers connected by αHL pores, but not when bilayers without pores interrupted the path (Figure 2d).

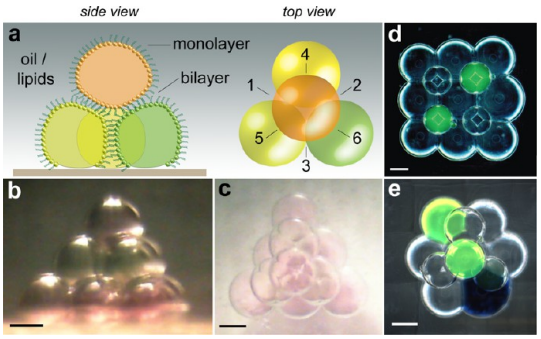

Figure 1. Three-dimensional networks of aqueous droplets connected with interface bilayers. (a) Cartoons showing a 3D droplet assembly (side view and top view). Lipid-coated droplets at the base support another lipid-coated droplet. The lipid monolayers form bilayers at the droplet−droplet interfaces (labeled 1−6). (b) Ten aqueous droplets in a three-layered network forming a pyramid (face-centered cubic) (side view); (c) top view. The light red (layer 1 and apex) and green droplets (layer 2) contained 5-carboxytetramethylrhodamine (5-cTAMRA) and fluorescein, respectively. Droplets could be placed in other lattice arrangements on patterned surfaces, (d) (100) (top view) and (e) hexagonal close packing (111) (top view). Here, some droplets contained 10 mM pyranine (green) or 100 mM xylene cyanol (blue). A mixture of hexadecane/silicone oil AR20 (1:1 v/v) containing 1 mg mL^{-1} DPhPC was used. In b and c, the DPhPC concentration inside the droplets was 1 mg mL^{-1}. In d, the lipid concentrations inside individual droplets varied (see Supporting Information Figure S5). Scale bars, 200 μm.

The magnitude of the total ionic current depended on the concentrations of αHL pores in the α and β droplets and whether intervening bilayers were present between these droplets. When droplet β was directly connected to droplet α, an exponential rise in the ionic current was observed (Figure 2f). If droplet β was then connected to a droplet without αHL (*cis* electrode) or to droplet α through one intervening droplet, a quantized increase in the ionic current was measured (cf. Figure 2f and 2g and Figure 2f and 2b,e, respectively). The increase in current arose from αHL pores in the two bilayers formed by the intervening droplet with droplets α and β, both of which contained αHL. To further prove that specific signals can be assigned to individual pathways, we used γCD to modulate the ionic current of one pathway. γCD binds within the β barrel of αHL, producing short current blockades.[20,21] The ionic current was intermittently interrupted when droplet β was connected to droplet α through a γCD-containing droplet (Figure 2h). The use of small molecules capable of blocking membrane pores could be a good way to impart signatures to different conductive pathways. Such a functional 3D droplet network, capable of transmitting electrical signals along defined branched pathways, may find applications in synthetic biology (*e.g.*, to mimic neuronal tissue)[19] and in engineering soft-matter devices with varied I/O (input−output) components in the same unit.[16]

Our next aim was to achieve chemical communication along predetermined pathways in a 3D network.

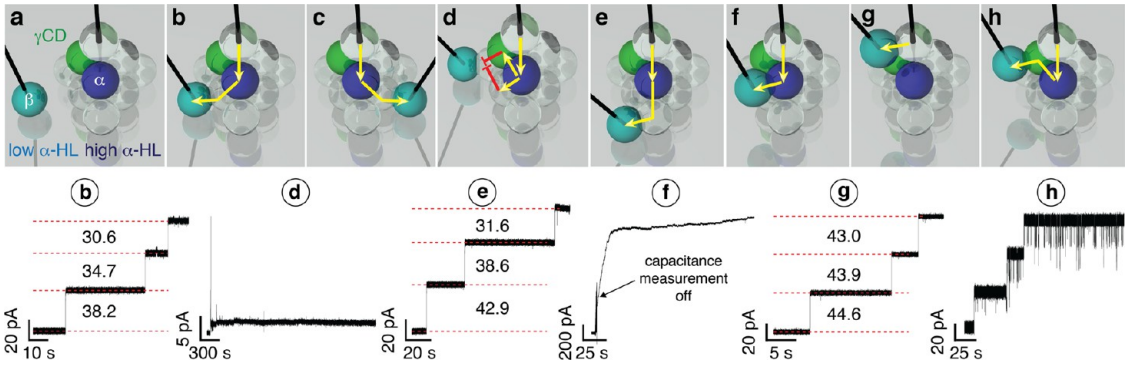

Figure 2. Directed communication between compartments of a 3D network. A 10-droplet pyramid was assembled layer-by-layer by injecting droplets (containing 1 mg mL^{-1} DPhPC liposomes) into a mixture of hexadecane/silicone oil containing DPhPC (1 mg mL^{-1}). The top panel shows cartoon representations of the 3D droplet network. (a) The Ag/AgCl electrode (*cis*) was inserted in the apical droplet after assembling the network. Two droplets (α, dark blue; β, cyan) contained αHL pores at ~830 and ~83 ng mL^{-1}, respectively. A third droplet (green) contained γCD (36 μM). "Probe" droplet β, at the end of a Ag/AgCl electrode (*trans*), was used to determine the path of ions through the network droplets measured as electrical signals (bottom panel). (b,c) Upon connecting droplets containing αHL (α and β) with one intervening empty droplet, αHL insertion was observed (bottom panel, corresponding representative current trace for b, c). The values between the red dotted lines denote the open pore currents (pA). (d) When α and β were connected through two empty droplets, there was no electrical connection as manifested by the absence of pore insertions. (e) When the probe droplet β was connected again to droplet α through a different intervening empty droplet at the lower vertex of the assembly, an electrical connection was re-established. (f) When β was connected directly to α (high concentration of αHL), a rapid increase in the current was observed instead of discrete insertion steps. (g) Droplet β was then connected to α through the top apex droplet as the intervening droplet. An ionic pathway was established but with a lower frequency of αHL insertions. (h) The electrical signal was interrupted by γCD blockades. Yellow and red arrows indicate open and blocked ionic pathways, respectively. The progressive decrease in the current amplitude with each insertion of αHL is expected, and its physical origin is explained in Figure S1. Images a−h in the top panel were created using POV-ray (http://www.povray.org).

This was demonstrated by diffusion of the hydrophilic, fluorescent dye pyranine in a 3D 14-droplet network with a square base. The four droplets at the vertices of a 3 × 3 base layer contained αHL heptamers. Four droplets containing αHL were placed on top of this layer, and finally, a pyranine-containing droplet was positioned on top of the entire structure (Figure 3a). Pyranine diffusion was observed from top to bottom, only through droplets containing αHL (Figure 3b−e). Current recordings confirmed that pyranine does not compromise bilayer stability (Figure S2), nor does it interfere with the assembly of αHL into the lipid bilayer (Figure S3). Chemical diffusion was also demonstrated in a 10-droplet pyramid assembly (Figure S4) and a 10-droplet network with a hexagonal base layer (Figure S5). These experiments demonstrate the construction of stable 3D droplet networks in which each droplet can contain different proteins or small molecules. The assemblies are functional units capable of internal and external communication.

Principle and Setup of Magnetic Assembly of Droplets. A key advance toward the fabrication of intricate synthetic tissues would be the ability to automate the construction of 3D droplet networks in a precisely controlled manner. To this end, we demonstrate that lipid-coated droplets can be manipulated with sub-millimeter precision by a magnet. We developed a levitation method to control the movement of a droplet with minimal disturbance to its neighbors (Figure 4a and Figure S6). Lipid-coated droplets, loaded with magnetic beads, were strewn on a polydimethylsiloxane (PDMS) surface patterned with pillars (Figure S6) to facilitate the precise arrangement of a first layer of droplets. The depth of the oil was adjusted such that the magnet, when brought close to the oil/air interface, produced a field just sufficient to lift one of the droplets to the interface. The surface tension of the oil prevented the aqueous droplet from breaking free from the oil phase. After positioning with the magnet, the levitated droplet was released by lifting the magnet away from the interface and thereby placed wherever desired on the patterned surface or on top of an existing 2D network to build a 3D structure (Figures 4a,b).

Magnetic Assembly and Manipulation of 2D Droplet Networks. By using the levitation technique, we first demonstrated the construction of a 2D network in which all the lipid-coated droplets contained magnetic beads. Three droplets (~400 nL) were moved separately with the magnetic rod and assembled in a triangular pattern. A flattened contact area between two droplets was a good indication of bilayer formation.[22] The assembly of droplets in such a manner yielded stable construction modules (CoM) (Figure 4d−g). That the droplets were attached to each other by stable interface bilayers was also proved by transportation of a CoM as a single unit. In one example, three 3-droplet CoMs were assembled to form a larger 9-droplet assembly (Figure 4g−k and movie S1). Next, we demonstrated the ease of transporting a complete droplet assembly (Figure S7). Seven droplets (~400 nL each) arranged in a floral pattern on a hexagonal dimpled surface were levitated and moved under a magnetic field. During transport, the

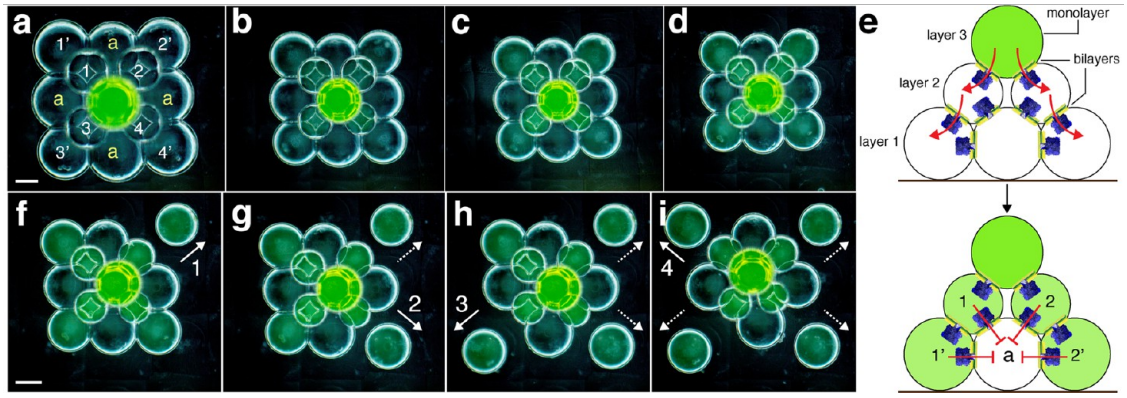

Figure 3. Specific communication pathways defined by αHL pores in a 3D droplet network. (a) A 9-droplet square array formed the bottom layer. The four droplets at the vertices (1′, 2′, 3′, 4′) contained heptameric αHL pores (~83 μg mL^{-1}). The droplets labeled "a" did not contain αHL. Four droplets (1, 2, 3, 4) containing αHL pores (~83 μg mL^{-1}) were placed with a pipet on the bottom layer to form a second layer, and finally, a droplet containing pyranine (10 mM) was placed on top of the assembly. (b) After 4 days, a color change was observed in all the droplets of the second layer. (c) After an additional ~12 h, the four vertex droplets of the base layer became green, turning darker after another 12 h (d). (e) Side view of a part of the droplet assembly (*i.e.*, the top droplet (green), droplets 1, 2, 1′, 2′, and droplet "a" between 1′ and 2′) showing the arrangement of the bilayers and the inserted αHL pores. The curved arrows (red) indicate pyranine diffusion from the top droplet (layer 3) to the droplets in layers 2 and 1. Subsequent diffusion from these droplets to the central edge droplets "a" of layer 1 was not observed. (f–i) The vertex droplets could be removed one-by-one without compromising the structural integrity of the remainder of the assembly. Because droplets "a" did not contain αHL, we reckon that the concentration of αHL pores in the bilayers formed between droplets 1 and "a", and similarly between 2, 1′, 2′, and "a", was lower than that between droplet pairs 1–1′, 2–2′, 3–3′, and 4–4′. Thus, on the timescale of the experiment, the fluorescence in droplet "a" did not increase as in the case of droplets 1, 2, 3, 4, 1′, 2′, 3′, and 4′. All the droplets contained DPhPC (1 mg mL^{-1}) and were assembled in a mixture of hexadecane/silicone oil AR20 containing DPhPC (2 mg mL^{-1}). Scale bars (a,f), 200 μm; (b–d) same scale as a; (g–i) same scale as f.

network's shape and bilayer connections were retained (movie S2).

The combined use of small, strong Nd magnets, a patterned surface, and adjustment of the height of the oil phase offers a way to remove specific droplets from a network and transfer them to another network (Figure S8). For example, the magnet was used to pull on a droplet using the PDMS pillars to produce resistance from the rest of an assembly. With this approach, we demonstrated the disassembly of a 2D network into its constituents (Figure S9 and movie S3). Droplets were peeled off starting with the outer ring. As the network size shrank, the decreasing resistance made disassembly of the last droplets difficult and they were left as a 3-droplet CoM (Figure S9). The maximum number of bilayers to which a droplet could be attached and still be removed from a 2D network was six (Figure S10a–c). Obviously, with decreasing magnetic field strength (*e.g.*, if the concentration of the magnetic particles inside a droplet is decreased), it will be difficult to overcome the resistance of the attached bilayers, thus limiting the utility of this approach in separating a droplet from its attached droplets.

To build droplet networks devoid of magnetic beads, we devised a so-called carrier droplet technique (see Methods). In brief, a droplet containing magnetic beads, used as the carrier droplet, was attached to an empty droplet through an interface bilayer (DIB). The two droplets were then connected to another empty droplet and subsequently to a third to form a CoM (Figure 5a–e and movie S4). To move the droplets with ease, a flat Petri dish surface was used instead of a patterned PDMS surface. In this case, since no patterned pillars were present to offer resistance, the carrier droplet was detached from the linear CoM by moving the magnet quickly (Figure 5f). [In this case, $F_{drag} > F_{bilayer}$, where F_{drag} is the drag force on the carrier droplet in oil, and $F_{bilayer}$ is the interaction force between the lipid monolayer of the carrier droplet and the droplet attached to it (Supplementary Note 2)]. Similarly, three droplets were arranged in a triangular pattern to give a second CoM, which was connected to the linear module to build a 2D 6-droplet triangle (Figure 5g–i and movie S4). The bilayer between the carrier droplet and the apex of the triangle withstood the drag force when the carrier droplet was used to move the entire assembly slowly (Figure 5j–m and movie S4). A network of empty droplets could be disassembled by fusing a droplet containing magnetic beads with an empty droplet and pulling it away from the rest of the assembly (Figure 6 and movie S5). To achieve fusion, lipids were absent from within the droplet containing the magnetic beads, and the concentration of lipids in the hexadecane was reduced to 0.5 mg mL^{-1}.

Recently, it was shown that an infrared laser could be used to move droplets in decanol and an oil phase to form bilayers.[23] The movement of these droplets was in the micrometer range and depended on the surfactant and the length of lipids used. Droplet fusion was achieved by positioning the laser spot on the bilayer. The use of a surfactant or heating is not ideal if proteins and cells are to be encapsulated inside the

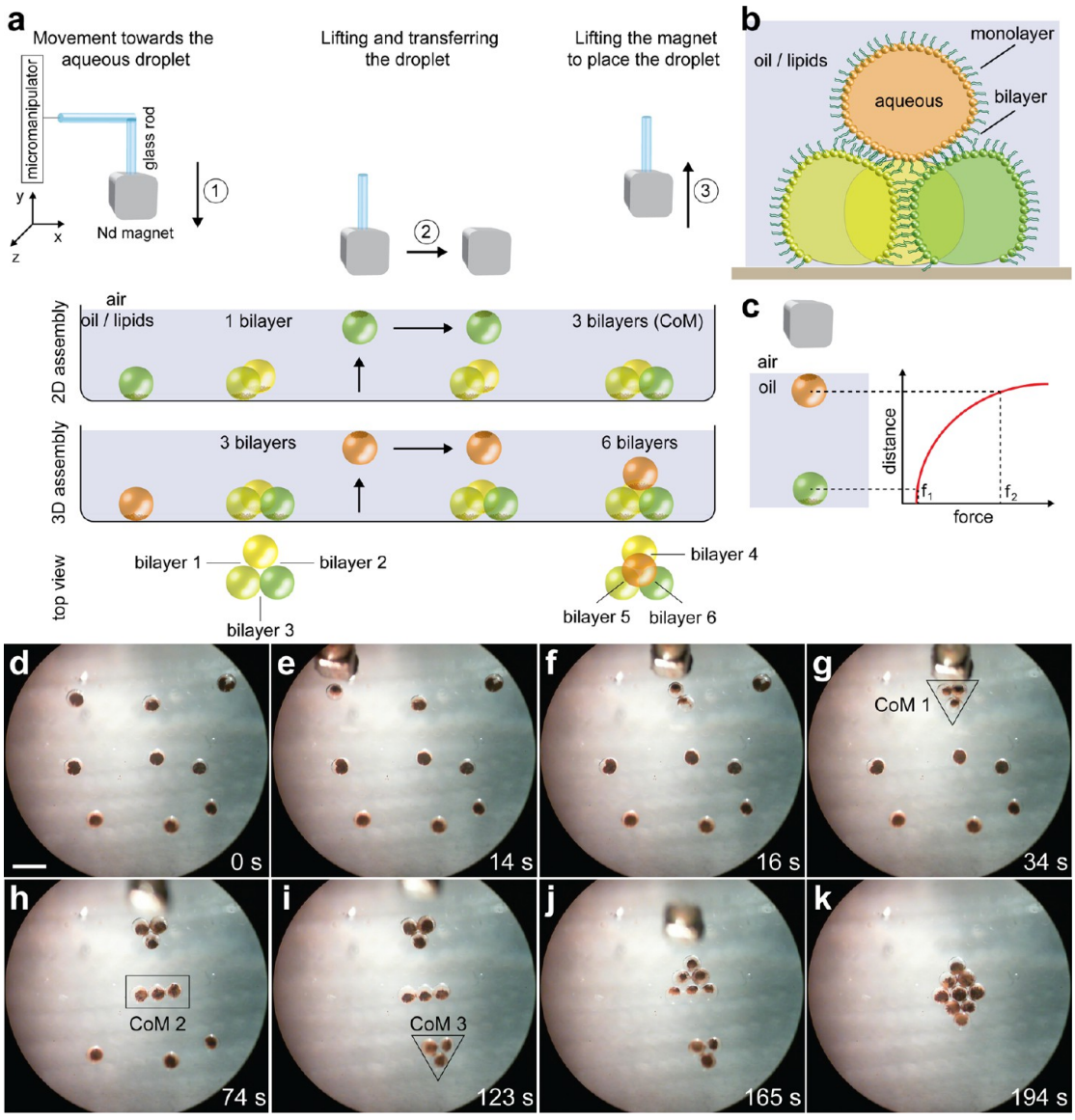

Figure 4. Construction of bilayer networks by droplet levitation. (a) Droplets containing lipids and magnetic beads were formed by injection into oil. A glass capillary with a Nd magnet glued to the end was attached to a *xyz* micromanipulator and used to move the droplets. A droplet was levitated by bringing the magnet close to the oil surface (step 1). The levitated droplet was moved laterally (step 2) and finally placed in a 2D bilayer network by lifting the magnet back to its original height (step 3). Similarly, placing droplets on a 2D network gave a 3D bilayer network (b). (c) The magnetic force experienced by a droplet decreased with its distance from the magnet ($f_1 < f_2$). The distance of the magnet from a droplet was therefore crucial in levitating the droplet without disturbing the droplets below. (d) Aqueous droplets (400 nL) containing both DPhPC liposomes and magnetic beads (see Methods) were strewn in a PDMS chamber with a surface patterned with pillars. The chamber was filled with DPhPC in hexadecane (1 mg mL^{-1}). (e–i) A Nd magnet was used to assemble the droplets into small construction modules (CoM 1, CoM 2, CoM 3) by using the levitating droplet technique. (j,k) The three modules were brought together to complete a 2D network (movie S1). The assembly was stable for at least 1 h. The elapsed time in seconds is shown. Scale bar (d), 2 mm (all panels at same scale).

droplets. Here, using a magnetic field, we were able to move droplets over tens of millimeters, precisely manipulate them, and by optimizing the lipid concentration, we achieved fusion between two droplets.

Magnetic Assembly and Manipulation of 3D Networks. In a first approach, a 3D bilayer network was constructed by assembling a 2D network of droplets containing magnetic particles and then placing additional magnetic droplets on the assembled 2D network by levitation (Figure S11 and movie S6). In a second approach, a three-layered 3D network was constructed with the bottom layer comprising empty droplets (made with the carrier droplet method), while the upper two droplet layers contained magnetic beads (assembled with the levitation technique) (Figure 7 and movie S7). The bilayer stability was high enough to avoid the slippage of upper droplets during translational motion of the networks (Figure S12). Interestingly, a 2D network can be converted to a 3D network by magnetically lifting a droplet and placing it on top of the

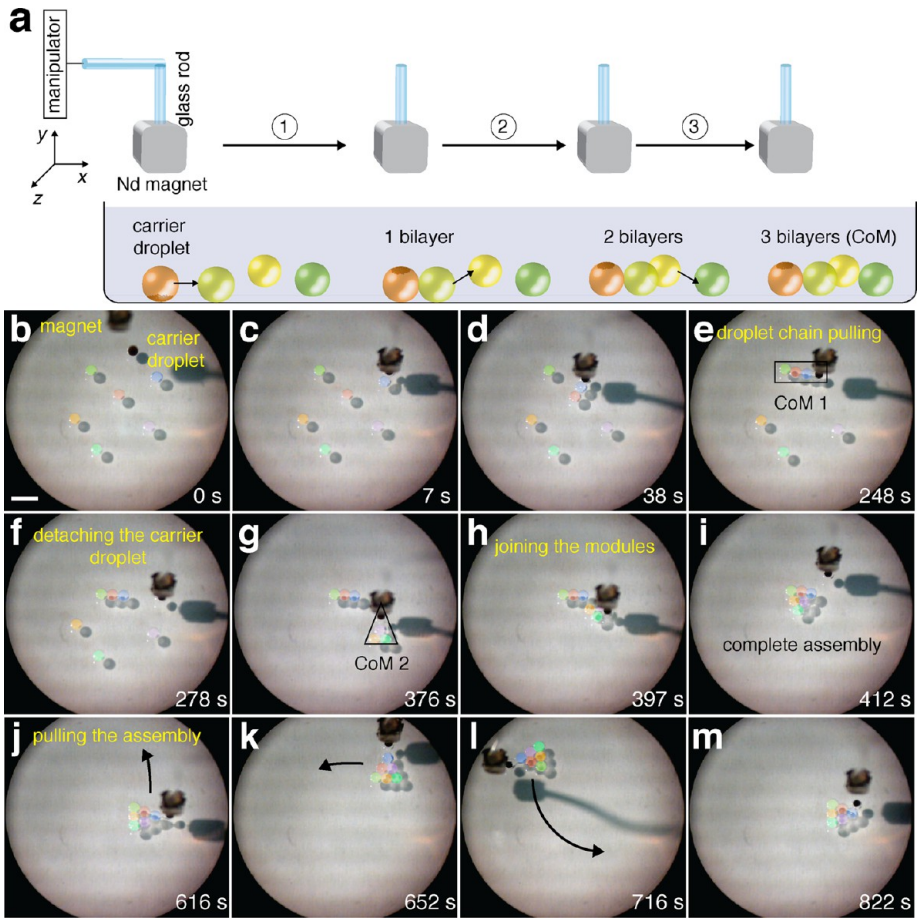

Figure 5. Two-dimensional network of empty droplets formed by the carrier droplet technique. (a) A two-dimensional droplet network was assembled on a polystyrene Petri dish by the carrier droplet method (see Methods). (b,c) The carrier droplet (loaded with magnetic beads) was moved to an empty droplet to form a DIB. (d,e) A linear chain of three empty droplets was formed as the first construction module (CoM 1). The bilayer between the carrier droplet and the linear droplet chain was strong enough to withstand the drag on the attached droplets while they were moved. (f) The carrier droplet was then detached from the linear droplet chain by moving the magnet quickly and used to form another module (CoM 2) with a triangular pattern (g). (h,i) CoM 1 and CoM 2 were connected to form a 6-droplet triangle. (j−m) The carrier droplet was used to pull the complete assembly around the dish (movie S4). All droplets were 400 nL in volume and contained DPhPC liposomes (1 mg mL^{-1}) in 1 M KCl, 10 mM Tris·HCl, pH 7.0. The oil phase was a mixture of hexadecane/silicone oil containing DPhPC (1 mg mL^{-1}). The gray spots are the shadows of the droplets. The droplets are false colored in Adobe Photoshop to enhance clarity. The elapsed time in seconds is shown. Scale bar (a), 2 mm (all panels at same scale).

rearranged bottom layer (Figure S13 and movie S8). By changing the droplet network topology in this way, it is possible to switch the electrical properties of a network.

The networks we have built in this work compare favorably with those constructed by other means. Two-dimensional manipulation of uncoated (*i.e.*, without a lipid monolayer) droplets has been demonstrated by using magnetic particles,[24,25] electrowetting,[26] and dielectrophoresis,[27] which has culminated in digital microfluidics.[28] In the context of connected droplets, dielectrophoresis has been used to move lipid-coated droplets in oil on pre-etched 2D tracks to form interface bilayers.[29] Conventional microfluidic approaches are routinely used to form and sort droplets in 2D.[30−32] Droplet pairs analogous to DIB were formed by employing a microfluidic droplet trap.[33] In the case of 3D construction, self-assembled 3D structures of oil droplets in water have been formed in specific crystallographic units, with distortion and defects.[34] Formation of two-layered DIB networks has been demonstrated using microfluidics.[35,36] Although this is an important step in the high-throughput generation of DIB networks, the networks were constrained within a microfluidic channel, thereby limiting the geometry of the networks and the ability to access and manipulate droplets once a network was formed. Recently, we showed that a printing device can be used to place lipid-stabilized droplets in a designed 3D network.[37] Albeit a good way to construct 3D networks, the technique poses the same problems of accessibility and manipulation of individual droplets once an assembly has been constructed. Also, the success of the printed network is mainly owed to the picoliter-sized droplets, which have sufficient time (tens of seconds) to assemble a lipid monolayer while falling from the glass capillary to

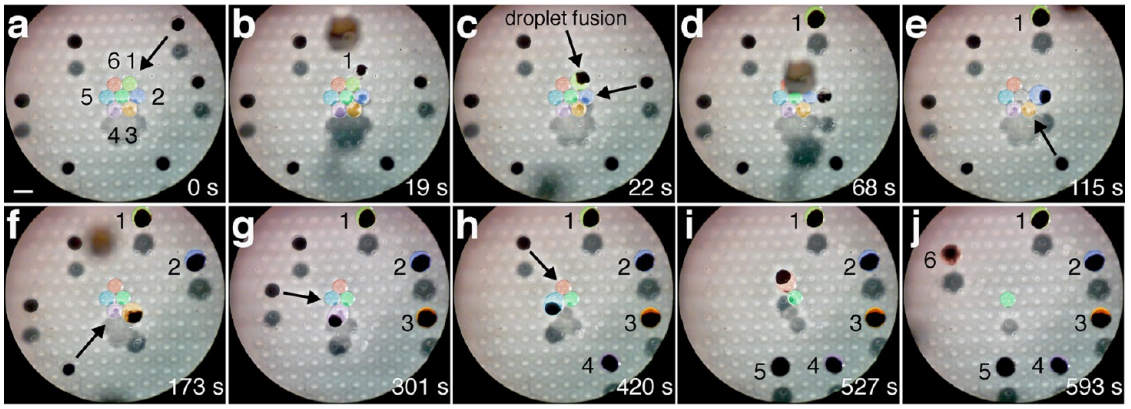

Figure 6. Disassembling a 2D network made of empty droplets. (a) A two-dimensional 7-droplet hexagon of empty 400 nL droplets (labeled 1−6, center droplet not labeled) was constructed on a patterned PDMS surface. (b−d) A magnetic carrier droplet was fused to empty droplet 1, and the droplet was peeled off the assembly by moving the magnet away. [We were unable to remove droplets from a 7-droplet hexagon network by the carrier droplet method, owing to the resistance experienced by the first droplet to be removed (three bilayers) and by the subsequent droplets (two bilayers)]. (e−j) The network was disassembled by sequentially removing the remaining empty droplets in a similar fashion (movie S5). To facilitate fusion between the magnetic carrier droplets and the empty network droplets, the DPhPC concentration in the hexadecane was reduced to 0.5 mg mL^{-1}, and no lipids were present in the magnetic droplet, enabling fusion in 3−69 s (n = 6). The concentration of DPhPC in the empty buffer droplets (1 M KCl, 10 mM Tris·HCl, pH 7.0) was 1 mg mL^{-1}. Decreasing the lipid concentration in the hexadecane did not compromise the stability of the droplet network. To enhance the clarity of the image, the droplets are false colored in Adobe Photoshop. Gray shadows of the droplets can be seen. The elapsed time in seconds is shown. Scale bar in (a), 1 mm (all panels at same scale).

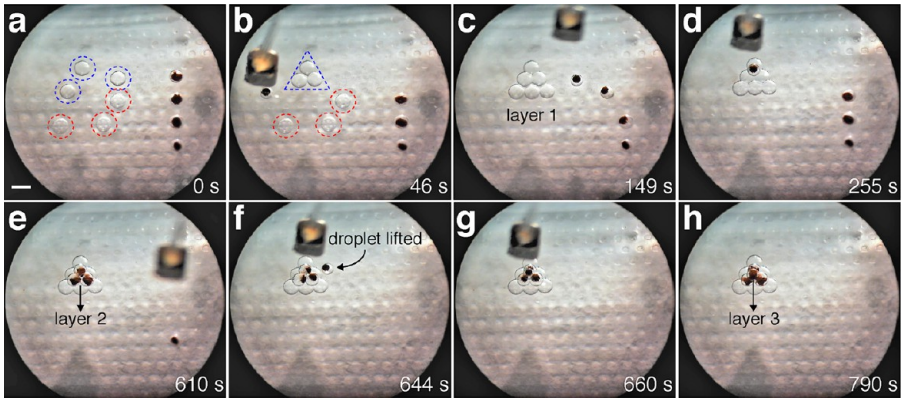

Figure 7. Three-dimensional network construction. A 3D assembly consisting of three droplet layers was constructed on a patterned PDMS surface. (a−c) The bottom layer (layer 1) was assembled by pushing individual droplets with a carrier droplet to form a 6-droplet triangle (circled dashed blue, assembled first, and red, assembled later). (d,e) Droplets loaded with magnetic beads were placed by levitation on layer 1 to form the 3-droplet layer 2. (f−h) The final droplet was lifted and placed (layer 3) on the second layer to finish the pyramidal assembly (movie S7). The elapsed time in seconds is shown. Scale bar in (a), 1 mm (all panels at same scale). Droplets from the two upper layers could be removed by magnetic levitation and placed back on the patterned surface, leaving behind a 2D assembly (Figure S11 and movie S6).

the bottom surface. Larger droplets (nL) require more time (>5 min) to accumulate lipid monolayers to form stable bilayers[13] and, therefore, cannot be used with printer devices to assemble 3D networks. In general, a current limitation of microfluidic or electrodynamic techniques[38] is that they cannot be used to pick a specific droplet from a palette and move it to a selected location in 3D space. To enhance the potential of droplets, it may be useful to develop methods for manipulating them in open space.[39] The current work demonstrates the first steps toward the manipulation of individual nanoliter-sized droplets from a 3D arrangement of droplets and an entire 3D assembly by using magnetic manipulation.

CONCLUSION AND OUTLOOK

Our long-term vision is to use lipid-coated droplet and hydrogel assemblies as models for synthetic minimal cells, prototissues, and functional devices.[16,37,40] In this regard, the assemblies are expected to perform various actions, such as energy storage and utilization, linear and rotary motion, sensing and signal transduction, the uptake, transformation and release of small molecules, and computation.[41] Compared to 2D assemblies, designed 3D networks of lipid-coated droplets are akin to biological tissues and can be programmed to perform specific functions.[37] The use of a magnetic field extends beyond simple manipulation of droplets

in 2D and 3D and can be used to realize some of the aforementioned goals.[40]

We envisage that 3D materials fabricated from hydrogels and droplets may find applications in bionanotechnology and synthetic biology because they can be controlled electronically,[16] with light[42] or by a magnetic field.[40] The ability to switch rapidly between droplet configurations does not occur naturally and will add to the versatility of synthetic minimal tissues (Figure S13). To build more complex synthetic tissues, programmed assembly is desirable. Computer-aided control of magnetic field in different steps of assembly and actuation[40] is a promising approach toward complete or partial automation.

METHODS

Wild-Type (WT) αHL Heptamer Preparation. The WT-αHL heptamer was produced by purifying spontaneously oligomerized αHL from *Staphylococcus aureus* Wood 46 cultures as described elsewhere.[43]

Droplet Interface Bilayer. Liposomes were prepared from 1,2-diphytanoyl-*sn*-glycero-3-phosphocholine (DPhPC) (Avanti Polar Lipids, USA) by extruding a hydrated lipid suspension (25 mg mL^{-1}) in 1 M KCl, 10 mM Tris·HCl, pH 7.0, through a polycarbonate membrane (pore size 0.1 μm). The liposomes were diluted in the same buffer to 1 mg mL^{-1} lipid. Submicroliter droplets (80−200 nL for manual assembly; 400−800 nL for magnetic assembly) of the diluted liposomes were injected into pure hexadecane (≥99%) (Sigma-Aldrich, UK) or hexadecane/silicone oil AR20 (Aldrich, UK) (1:1 v/v). Depending on the lipid concentration in the oil phase, and the type of oil used, the droplets were incubated from ∼5 to 30 min. During this period, they became encased in a lipid monolayer. When two lipid-encased droplets are brought together, a bilayer formed at the interface. Aqueous droplets in the hexadecane/silicone oil mixture (1:1 v/v) needed less time (5−10 min) to form stable bilayers than they did in pure hexadecane (≥30 min).

3D Network Formation. To form robust 3D droplet networks, bilayers stable for hours to days were required. Different ratios of silicone oil AR20 and hexadecane were tested. A composition was deemed suitable if it promoted the fast formation of bilayers upon bringing two droplets together (as determined by monitoring an increase in the capacitance) and if the bilayers were stable with and without an applied potential (up to +200 mV). To form 3D networks, a 1:1 (v/v) mixture of hexadecane and silicone oil AR20 containing 1 mg mL^{-1} DPhPC lipids was used. The aqueous droplets contained DPhPC liposomes (1 mg mL^{-1}) in 1 M KCl, 10 mM Tris·HCl, pH 7.0. Dye diffusion experiments were performed with droplets containing 10 mM pyranine (8-hydroxypyrene-1,3,6-trisulfonic acid) (Invitrogen) and 100 mM xylene cyanol FF (Sigma-Aldrich) dissolved in 1 M KCl, 10 mM Tris·HCl, pH 7.0, containing DPhPC liposomes (1 mg mL^{-1}). Aqueous droplets were pipetted into oil and incubated for up to 30 min to form a lipid monolayer coat. One or more droplets were then sucked into a pipet tip along with a small amount of oil and placed close to each other by pipetting out to form a 2D base layer. Incubated droplets were pipetted on the base layer to obtain a 3D network.

Electrical Recordings. A Ag/AgCl electrode, the *cis* electrode, was inserted into one droplet and attached to the grounded end of a patch-clamp headstage (Axon Instruments, USA). A second Ag/AgCl electrode (*trans*) inserted in another droplet was connected to the active end. A positive potential causes the flow of anions from the *cis* to the *trans* electrode and of cations from *trans* to *cis*. The current was amplified by using a patch-clamp amplifier (Axopatch 200B, Axon Instruments, USA), filtered with a low-pass Bessel filter (80 dB/decade) with a corner frequency of 1 kHz, and digitized with a Digidata 1322 A/D converter (Axon Instruments) at a sampling frequency of 20 kHz. Postacquisition, the data were low-pass-filtered at 100 to 400 Hz. The droplet assembly, electrodes, and the headstage were enclosed in a metal box to minimize electrical noise.

Setup for Magnetic Manipulation. A Nd magnet (1.2 mm × 1.2 mm × 1.2 mm) (Magnet Expert Ltd., UK) was stuck to the end of a glass capillary (0.5 mm o.d.) (Figure S6), which was attached to a micromanipulator (World Precision Instruments, UK). The capillary was used to manipulate the droplets. Ni-NTA magnetic beads (MagneHis Ni-particles, Promega, USA) were mixed with buffer (1 M KCl, 10 mM Tris·HCl, pH 7.0) containing liposomes (1 mg mL^{-1} DPhPC) in a ratio of 1:2 (v/v). Droplets (400 nL) were formed by injecting this mixture into hexadecane or hexadecane/silicone oil containing DPhPC (1 mg mL^{-1}). The lipid concentration in the aqueous and oil phases was the same in all experiments, unless stated otherwise.

Patterned Surface Features. Small pillars were patterned in a hexagonal array on a PDMS surface and used to keep droplets stationary (Figure S6). The dimensions of the pillars were 0.4 mm × 0.2 mm (diameter × height), and the center-to-center distance was 0.7 mm. The patterned PDMS was made by pouring Sylgard 184 silicone elastomer (Dow Corning, USA) onto a poly(methyl methacrylate) (PMMA) mold in a polystyrene Petri dish and heating the dish at 80 to 90 °C to induce polymerization.

To form droplet networks, the PDMS was covered with oil at a depth 1 to 3 times the height of the droplets. The droplets sat on the patterned surface so that adjacent droplets were in contact with each other. As the magnet was brought close to the droplets, the force on the target droplet was sufficient to lift it over the pillars. The droplets on either side experienced a smaller magnetic force insufficient to overcome the pillar barriers. Therefore, this method allowed droplets to be individually extracted from a network.

Levitating Droplet Technique. The density of hexadecane/silicone oil mixture is ∼0.9 times the density of water. We estimate that a 400 nL droplet will experience an upward buoyant force of 3.5 μN. When a magnetic force was applied, the droplets rose closer to the magnet and experienced a progressively increasing force. The depth of the oil was adjusted so that the magnet did not touch the surface, and the field strength at the oil/air interface was insufficient for the droplet to overcome the surface tension. Therefore, the droplet remained fully immersed. An elevated droplet traveled with the magnet when it was moved with the *xyz* manipulator, while a negligible force was exerted on the droplets resting beneath. By lifting the magnet, the elevated droplet could be dropped at a desired location and inserted into a network with good spatial resolution without disturbing the neighboring droplets.

Carrier Droplet Technique. A droplet (400 nL or 800 nL) containing magnetic beads was used to pull several smaller nonmagnetic droplets (400 nL) connected by interface bilayers (Figure 5). The magnetic droplet could be detached from the other droplets by pulling it quickly (on a flat unpatterned surface) to break the bilayer. To move droplets on a surface, friction was minimized by using a hydrophobic PDMS surface or the surface of a new polystyrene Petri plate.

Conflict of Interest: The authors declare no competing financial interest.

Acknowledgment. This work was funded by the MRC. K.T.S. was supported by a Marie Curie Intra-European fellowship. T.W. was supported by the German National Academic Foundation (Studienstiftung des Deutschen Volkes), H.G. by an EMBO long-term fellowship, S.M. by a Clarendon Fund Scholarship, and J.H. was funded by an EPSRC Life Sciences Interface Doctoral Training Centre studentship.

Supporting Information Available: Additional information on electrical characterization of 3D droplet assemblies, lipid bilayers, dye diffusion in the assemblies, and formation and manipulation of 3D droplet assemblies using a magnetic field. This material is available free of charge *via* the Internet at http://pubs.acs.org.

REFERENCES AND NOTES

1. Song, H.; Chen, D. L.; Ismagilov, R. F. Reactions in Droplets in Microfluidic Channels. *Angew. Chem., Int. Ed.* **2006**, *45*, 7336–7356.
2. Griffiths, A. D.; Tawfik, D. S. Miniaturising the Laboratory in Emulsion Droplets. *Trends Biotechnol.* **2006**, *24*, 395–402.
3. Pipper, J.; Inoue, M.; Ng, L.; Neuzil, P.; Novak, L. Catching a Bird Flu in a Droplet. *Nat. Med.* **2007**, *13*, 1259–1263.
4. Fallah-Araghi, A.; Baret, J.-C.; Ryckelyncka, M.; Griffiths, A. D. A Completely *In Vitro* Ultrahigh-Throughput Droplet-Based Microfluidic Screening System for Protein Engineering and Directed Evolution. *Lab Chip* **2012**, *12*, 882–891.
5. Loakes, D.; Holliger, P. Darwinian Chemistry: Towards the Synthesis of a Simple Cell. *Lab Chip* **2009**, *5*, 686–694.
6. Schrum, J. P.; Zhu, T. F.; Szostak, J. W. The Origins of Cellular Life. *Cold Spring Harbor Perspect. Biol.* **2010**, *2*, a002212.
7. Agresti, J. J.; Antipov, E.; Abate, A. R.; Ahn, K.; Rowat, A. C.; Baret, J.-C.; Marquez, M.; Klibanov, A. M.; Griffiths, A. D.; Weitz, D. A. Ultrahigh-Throughput Screening in Drop-Based Microfluidics for Directed Evolution. *Proc. Natl. Acad. Sci. U.S.A.* **2010**, *107*, 4004–4009.
8. Tawfik, D. S.; Griffiths, A. D. Man-Made Cell-like Compartments for Molecular Evolution. *Nature* **1998**, *16*, 652–656.
9. Vogel, S. K.; Schwille, P. Minimal Systems To Study Membrane–Cytoskeleton Interactions. *Curr. Opin. Biotechnol.* **2012**, *23*, 758–765.
10. Szostak, J. W.; Bartel, D. P.; Luisi, P. L. Synthesizing Life. *Nature* **2001**, *409*, 387–390.
11. Noireaux, V.; Libchaber, A. A Vesicle Bioreactor as a Step toward an Artificial Cell Assembly. *Proc. Natl. Acad. Sci. U.S. A.* **2004**, *101*, 17669–17674.
12. Chiarabelli, C.; Stano, P.; Luisi, P. L. Chemical Approaches to Synthetic Biology. *Curr. Opin. Biotechnol.* **2009**, *20*, 492–497.
13. Holden, M. A.; Needham, D.; Bayley, H. Functional Bionetworks from Nanoliter Water Droplets. *J. Am. Chem. Soc.* **2007**, *129*, 8650–8655.
14. Syeda, R.; Holden, M. A.; Hwang, W. L.; Bayley, H. Rapid Screening of Blockers Against a Potassium Channel with a Droplet Interface Bilayer Array. *J. Am. Chem. Soc.* **2008**, *130*, 15543–15548.
15. Bayley, H.; Cronin, B.; Heron, A.; Holden, M. A.; Hwang, W. L.; Syeda, R.; Thompson, J. B.; Wallace, M. Droplet Interface Bilayers. *Mol. BioSyst.* **2008**, *4*, 1191–1208.
16. Maglia, G.; Heron, A. J.; Hwang, W. L.; Holden, M. A.; Mikhailova, E.; Li, Q.; Cheley, S.; Bayley, H. Droplet Networks with Incorporated Protein Diodes Show Collective Properties. *Nat. Nanotechnol.* **2009**, *4*, 437–440.
17. Noireaux, V.; Maeda, Y. T.; Libchaber, A. Development of an Artificial Cell, from Self-Organization to Computation and Self-Reproduction. *Proc. Natl. Acad. Sci. U.S.A.* **2011**, *108*, 3473–3480.
18. Woolfson, D. N.; Bromley, E. H. C. Synthetic Biology: A Bit of Rebranding, or Something New and Inspiring? *Biochemist* **2011**, *33*, 19–25
19. Villar, G.; Heron, A. J.; Bayley, H. Formation of Droplet Networks That Function in Aqueous Environments. *Nat. Nanotechnol.* **2011**, *6*, 803–808.
20. Gu, L.-Q.; Cheley, S.; Bayley, H. Capture of a Single Molecule in a Nanocavity. *Science* **2001**, *291*, 636–640.
21. Gu, L. Q.; Braha, O.; Conlan, S.; Cheley, S.; Bayley, H. Stochastic Sensing of Organic Analytes by a Pore-Forming Protein Containing a Molecular Adapter. *Nature* **1999**, *398*, 686–690.
22. Heron, A. J.; Thompson, J. R.; Mason, A. E.; Wallace, M. I. Direct Detection of Membrane Channels from Gels Using Water-In-Oil Droplet Bilayers. *J. Am. Chem. Soc.* **2007**, *129*, 16042–16047.
23. Dixit, S. S.; Kim, H.; Vasilyev, A.; Eid, A.; Faris, G. W. Light-Driven Formation and Rupture of Droplet Bilayers. *Langmuir* **2010**, *26*, 6193–6200.
24. Egatz-Gómez, A.; Melle, S.; García, A. A.; Lindsay, S. A.; Márquez, M.; Domínguez-García, P.; Rubio, M. A.; Picraux, S. T.; Taraci, J. L.; Clement, T.; *et al.* Discrete Magnetic Microfluidics. *Appl. Phys. Lett.* **2006**, *89*, 034106.
25. Gijs, M. A.; Lacharme, F.; Lehmann, U. Microfluidic Applications of Magnetic Particles for Biological Analysis and Catalysis. *Chem. Rev.* **2010**, *110*, 1518–1563.
26. Pollack, M. G.; Shenderov, A. D.; Fair, R. B. Electrowetting-Based Actuation of Droplets for Integrated Microfluidics. *Lab Chip* **2002**, *2*, 96–101.
27. Gascoyne, P. R. C.; Vykoukal, J. V.; Schwartz, J. A.; Anderson, T. J.; Vykoukal, D. M.; Current, K. W.; McConaghy, C.; Beckera, F. F.; Andrewsd, C. Dielectrophoresis-Based Programmable Fluidic Processors. *Lab Chip* **2004**, *4*, 299–309.
28. Choi, K.; Ng, A. H. C.; Fobel, R.; Wheeler, A. R. Digital Microfluidics. *Annu. Rev. Anal. Chem.* **2012**, *5*, 413–440.
29. Aghdaei, S.; Sandison, M. E.; Zagnoni, M.; Green, N. G.; Morgan, H. Formation of Artificial Lipid Bilayers Using Droplet Dielectrophoresis. *Lab Chip* **2008**, *8*, 1617–1620.
30. Whitesides, G. M. The Origins and the Future of Microfluidics. *Nature* **2006**, *442*, 368–373.
31. Weibel, D. B.; Whitesides, G. M. Applications of Microfluidics in Chemical Biology. *Curr. Opin. Chem. Biol.* **2006**, *10*, 584–591.
32. Theberge, A. B.; Courtois, F.; Schaerli, Y.; Fischlechner, M.; Abell, C.; Hollfelder, F.; Huck, W. T. Microdroplets in Microfluidics: An Evolving Platform for Discoveries in Chemistry and Biology. *Angew. Chem., Int. Ed.* **2010**, *49*, 5846–5868.
33. Bai, Y.; He, X.; Liu, D.; Patil, S. N.; Bratton, D.; Huebner, A.; Hollfelder, F.; Abell, C.; Huck, W. T. A Double Droplet Trap System for Studying Mass Transport Across a Droplet–Droplet Interface. *Lab Chip* **2010**, *10*, 1281–1285.
34. Shui, L.; Kooij, E. S.; Wijnperle, D.; van den Berg, A.; Eijkel, J. C. T. Liquid Crystallography: 3D Microdroplet Arrangements Using Microfluidics. *Soft Matter* **2009**, *5*, 2708–2712.
35. Stanley, C. E.; Elvira, K. S.; Niu, X. Z.; Gee, A. D.; Ces, O.; Edel, J. B.; deMello, A. J. A Microfluidic Approach for High-Throughput Droplet Interface Bilayer (DIB) Formation. *Chem. Commun.* **2010**, *46*, 1620–1622.
36. Elani, Y.; deMello, A. J.; Niu, X.; Ces, O. Novel Technologies for the Formation of 2D and 3D Droplet Interface Bilayer Networks. *Lab Chip* **2012**, *12*, 3514–3520.
37. Villar, G.; Graham, A. D.; Bayley, H. A Tissue-like Printed Material. *Science* **2013**, *340*, 48–52.
38. Velev, O. D.; Prevo, B. G.; Bhatt, K. H. On-Chip Manipulation of Free Droplets. *Nature* **2003**, *426*, 515–516.
39. Kaigala, G. V.; Lovchik, R. D.; Delamarche, E. Microfluidics in the "Open Space" for Performing Localized Chemistry on Biological Interfaces. *Angew. Chem., Int. Ed.* **2012**, *51*, 11224–11240.
40. Sapra, K. T.; Bayley, H. Lipid-Coated Hydrogel Shapes as Components of Electrical Circuits and Mechanical Devices. *Sci. Rep.* **2012**, *2*, 848.
41. Astier, Y.; Bayley, H.; Howorka, S. Protein Components for Nanodevices. *Curr. Opin. Chem. Biol.* **2005**, *9*, 576–584.
42. Punnamaraju, S.; You, H.; Steckl, A. J. Triggered Release of Molecules Across Droplet Interface Bilayer Lipid Membranes Using Photopolymerizable Lipids. *Langmuir* **2012**, *28*, 7657–7664.
43. Maglia, M.; Henricus, M.; Wyss, R.; Li, Q.; Cheley, S.; Bayley, H. DNA strands from denatured duplexes are translocated through engineered protein nanopores at alkaline pH. *Nano Lett.* **2009**, *9*, 3831–3836.